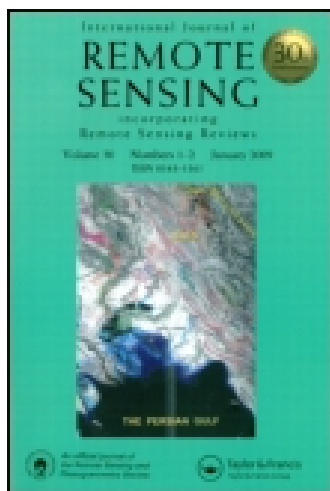


This article was downloaded by: [Eindhoven Technical University]

On: 17 February 2015, At: 00:05

Publisher: Taylor & Francis

Informa Ltd Registered in England and Wales Registered Number: 1072954 Registered office: Mortimer House, 37-41 Mortimer Street, London W1T 3JH, UK



International Journal of Remote Sensing

Publication details, including instructions for authors and subscription information:

<http://www.tandfonline.com/loi/tres20>

Retrieving parameters of bare soil surface roughness and soil water content under arid environment from ERS-1, -2 SAR data

Arthur Genis^{a b}, Leonid Vulfson^{b c}, Dan G. Blumberg^a, Michael Sprinstin^{a d}, Alexey Kotlyar^c, Valentine Freilikher^c & Jiftah Ben-Asher^{a b d}

^a Department of Geography and Environmental Development, Ben Gurion University of the Negev, Beer-Sheva, Israel

^b Katif Research Centre for the Development of Coastal Deserts, Israel

^c Department of Physics, Bar-Ilan University, Tel-Aviv, Israel

^d Jacob Blaustein Institute for Desert Research, Ben Gurion University of the Negev, Beer-Sheva, Israel

Published online: 24 May 2013.

To cite this article: Arthur Genis, Leonid Vulfson, Dan G. Blumberg, Michael Sprinstin, Alexey Kotlyar, Valentine Freilikher & Jiftah Ben-Asher (2013) Retrieving parameters of bare soil surface roughness and soil water content under arid environment from ERS-1, -2 SAR data, International Journal of Remote Sensing, 34:17, 6202-6215, DOI: [10.1080/01431161.2013.793862](https://doi.org/10.1080/01431161.2013.793862)

To link to this article: <http://dx.doi.org/10.1080/01431161.2013.793862>

PLEASE SCROLL DOWN FOR ARTICLE

Taylor & Francis makes every effort to ensure the accuracy of all the information (the "Content") contained in the publications on our platform. However, Taylor & Francis, our agents, and our licensors make no representations or warranties whatsoever as to the accuracy, completeness, or suitability for any purpose of the Content. Any opinions and views expressed in this publication are the opinions and views of the authors, and are not the views of or endorsed by Taylor & Francis. The accuracy of the Content should not be relied upon and should be independently verified with primary sources of information. Taylor and Francis shall not be liable for any losses, actions, claims, proceedings, demands, costs, expenses, damages, and other liabilities whatsoever or

howsoever caused arising directly or indirectly in connection with, in relation to or arising out of the use of the Content.

This article may be used for research, teaching, and private study purposes. Any substantial or systematic reproduction, redistribution, reselling, loan, sub-licensing, systematic supply, or distribution in any form to anyone is expressly forbidden. Terms & Conditions of access and use can be found at <http://www.tandfonline.com/page/terms-and-conditions>

Retrieving parameters of bare soil surface roughness and soil water content under arid environment from ERS-1, -2 SAR data

Arthur Genis^{a,b*}, Leonid Vulfson^{b,c}, Dan G. Blumberg^a, Michael Sprinstin^{a,d}, Alexey Kotlyar^c, Valentine Freilikher^c, and Jiftah Ben-Asher^{a,b,d}

^aDepartment of Geography and Environmental Development, Ben Gurion University of the Negev, Beer-Sheva, Israel; ^bKatif Research Centre for the Development of Coastal Deserts, Israel; ^cDepartment of Physics, Bar-Ilan University, Tel-Aviv, Israel; ^dJacob Blaustein Institute for Desert Research, Ben Gurion University of the Negev, Beer-Sheva, Israel

(Received 14 July 2011; accepted 10 December 2012)

Evaluation of the environmental and agricultural potential of arid lands is often limited by the lack of information on soil surface roughness and water content. The current study proposes an efficient method to retrieve these parameters of bare soil from single-channel ERS-1, -2 synthetic aperture radar (SAR) data. New equations were derived by combining the model for vertically co-polarized mode backscattering coefficient σ_{vv}^0 , the model for the real part of dielectric constant ϵ , and the empirical equation interrelating parameters of roughness. These equations allowed for calculation of the root mean square (RMS) height h of small surface roughness ($h \leq 1$ cm) for naturally sandy, flat areas of the Negev desert (Israel) during dry periods when θ is extremely low and generally known. As soil roughness was found to be sufficiently constant under the arid environment, this study showed that calculated h could be reliably used to retrieve θ during the wet period. Statistical analysis of the relative errors of retrieved h and θ showed their high independence on the absolute values. Retrieved values of h and θ obtained from ERS-2 SAR data showed acceptable correlation with the direct ground measurements. Therefore, the effectiveness of the proposed methodology for h and θ retrieval was proved.

1. Introduction

Surface soil roughness parameters (root mean square (RMS) height, h , and correlation length, l) and soil water content, θ , are important parameters influencing rainfall distribution among runoff, evaporation, and infiltration. They are also important in determining the surface energy balance which governs the partitioning between latent and sensible heat (Sud et al. 1990; Carmi and Berliner 2008). From a practical standpoint, these parameters are important determinants of aeolian erosion and deposition, which are intimately related to desertification and deterioration of agricultural lands in arid environments (Blumberg and Greeley 1993; Rees and Arnold 2007).

Information on spatial and temporal distribution of θ is important for environmental monitoring and evaluation of the suitability of undisturbed lands for arid agriculture. However, since continuous monitoring of rainfall and θ by conventional ground methods is expensive and time consuming, rapid and inexpensive mapping and monitoring methods

*Corresponding author. Email: argenis@bgu.ac.il

are needed for this purpose, especially in the Negev desert region of southern Israel, where extensive undisturbed lands exist with the potential for conversion to agriculture.

Remote sensing in the microwave range is such an effective method for retrieving soil moisture information because the detected microwave signal is greatly influenced by the dielectric properties of soil, which are a function of the soil water content (Ulaby, Moore, and Fung 1986; Peplinski, Ulaby, and Dobson 1995; Blumberg, Freilikh, Ben-Asher, et al. 2006; Blumberg, Freilikh, Kaganovskii, et al. 2006; Verhoest et al. 2008). For environmental monitoring, space-borne platforms are preferred since these allow surveying at regular time intervals. Space systems with active microwave imaging sensors having the required spatial resolution for capturing small-scale soil moisture patterns are available. Synthetic aperture radar (SAR) is the most suitable tool among these.

Various empirical, semi-empirical, and theoretical models have been developed relating the backscattering coefficient σ^0 to θ , h , and l . These models are used to calculate either θ or roughness parameters (Fung and Chen 2004; Walker et al. 2004; Verhoest et al. 2008). In most cases, h is the main parameter used in radar backscattering models for retrieving values of surface soil moisture content from radar images. Some studies on determination of surface roughness by remote sensing use θ values obtained from direct ground measurements as an input (Lin 1994; Walker et al. 2004). Other studies rely on time series solutions which follow the changes of σ^0 and assume no modification of target variables such as soil texture and roughness (Blyth 1997; Moran et al. 2000; Blumberg, Freilikh, Kaganovskii, et al. 2006). There are also methods based on multiple imaging in various domains (polarization, wavelength, λ , or incident angle, θ_1) in order to separate the relative impact of roughness and water content on backscattering (Oh, Sarabandi, and Ulaby 1992; Oh, Sarabandi, and Ulaby 1994; Dubois, Van Zyl, and Engman 1995; Bindlish and Barros 2000; Blumberg and Freilikh 2001; Zribi, et al. 2005; Baghdadi, Holah, and Zribi 2006; Blumberg, Freilikh, Ben-Asher, et al. 2006; Baghdadi et al. 2007; Baghdadi et al. 2008; Verhoest et al. 2008; Gherboudj et al. 2011).

Many studies on environmental change require time series data on soil moisture, but this information is often lacking. Archive data from the European Remote Sensing (ERS) satellite have been collected since 1991 and have the potential to provide time series data on soil moisture. Estimation of θ from single-channel ERS SAR data, however, requires concurrent measurements of h whereas estimation of h requires measurements of θ .

The objective of this study was to solve the above problem by developing a new method that uses certain unique qualities of arid lands. According to Carmi and Berliner (2008), rainfall has no effect on surface roughness when $h < 0.7$ cm. Moreover, the surface roughness of natural arid ecosystems does not change significantly with time (Verhoest et al. 1998; Moran et al. 2000; Walker et al. 2004; Álvarez-Mozos et al. 2006; Thoma et al. 2006; Verhoest et al. 2008). In addition, during the dry period (June–October), θ is extremely low (corresponding to air-dried soil), varies insignificantly, and is generally known. Therefore, the laborious estimation of θ required for retrieval of h can be avoided.

The method developed utilizes a combination of three models: (1) the semi-empirical model of Oh, Sarabandi, and Ulaby (1994) for vertically co-polarized mode backscattering coefficient, σ_{vv}^0 , of bare surfaces; (2) the empirical equation of Baghdadi et al. (2004), which derives the correlation length of roughness, l , as a function of h ; and (3) the semi-empirical model of Peplinski, Ulaby, and Dobson (1995) for the dielectric constant, ϵ . Values of h obtained during drought conditions were used for θ retrieval during wet conditions. To validate the output, h and θ determined by conventional ground methods were compared with h and θ determined by the remote method developed.

2. Materials and methods

2.1. New modeling method for the retrieval of h and θ

The semi-empirical backscattering model of Oh, Sarabandi, and Ulaby (1994) is based on several existing theoretical backscattering models (Ulaby, Moore, and Fung 1986), in conjunction with extensive experimental data. It is an extension of an empirical model (Oh, Sarabandi, and Ulaby 1992) and includes both magnitude and phase of the backscattering. The experimental data used to solve for the unknown constants were collected from a truck-mounted L-, C-, and X-band polarimetric scatterometer over a range of incidence angles from 10° to 70° . Surface roughness covered the ranges $0.1 < h < 5.0$ cm and $2.0 < l < 18.0$ cm. The model calculates vertically co-polarized (VV) mode backscattering coefficient, σ_{vv}^0 , as a function of h (cm), l (cm), θ , λ (cm), and θ_1 (rad).

The empirical equation of Baghdadi et al. (2004), developed for the calibration of theoretical integral equation model (IEM) of Fung (1994) with reference to ERS-2 SAR data, was also found to be suitable for the semi-empirical backscattering model calibration used in this study. According to Baghdadi et al. (2004), under given conditions, correlation length, l , as a function of h can be written as a power-type relationship:

$$l = \varphi h^\xi, \quad (1)$$

where ξ and φ are fitting constants ($\xi = 0.88$, $\varphi = 15.22$ cm) obtained from an independent set of ground-measured h and remote sensing σ_{vv}^0 data to ensure a better agreement between modelled and experimental σ_{vv}^0 values.

In the model of Oh, Sarabandi, and Ulaby (1994), the dielectric constant, ε , of the soil can be expressed through θ (% by volume), employing the widely used soil–water–air dielectric mixing model of Peplinski, Ulaby, and Dobson (1995). It has validity for bands K, X, C, and L and accounts for the most important factors including observation frequency (Hz), soil texture (fractions of sand and clay), and temperature, T ($^\circ\text{C}$).

To build the new model, given sets of h (0.1–1.0 cm, step 0.05 cm) and θ (1–30% by volume, step 1% by volume) were used as input to the models of Oh, Sarabandi, and Ulaby (1994) and Peplinski, Ulaby, and Dobson (1995) and Equation (1) under constant $\theta_1 = 23^\circ$, $\lambda = 5.65$ cm, $T = 10, 20, \text{ and } 30^\circ\text{C}$ for both sand and sandy loam. A set of σ_{vv}^0 values (dB) corresponding to each pair of h and θ was obtained as output. Numerical analysis of all received σ_{vv}^0 showed that h could be fitted as a function of σ_{vv}^0 and θ with high precision ($R^2 \geq 0.999$, residual mean square error (RMSe) ≤ 0.01 cm). As a result, the following equation was acquired:

$$h = e^{b(\theta)(\sigma_{vv}^0 + c(\theta))}, \quad (2)$$

where b is a second-degree polynomial fitting function of θ :

$$b = \alpha_0 + \alpha_1\theta + \alpha_2\theta^2, \quad (3)$$

c is a logarithmic fitting function of θ :

$$c = k \ln \theta + \mu, \quad (4)$$

and $\alpha_0, \alpha_1, \alpha_2, k$, and μ are fitting parameters.

Analogously, θ could be fitted as a function of σ_{vv}^0 and h ($R^2 \geq 0.991$, $\text{RMSe} \leq 0.06\%$ by volume):

$$\theta = e^{b_1(h)(\sigma_{vv}^0 + c_1(h))}, \quad (5)$$

where b_1 is a second-degree polynomial fitting function of h :

$$b_1 = \beta_0 + \beta_1 h + \beta_2 h^2, \quad (6)$$

c_1 is a logarithmic fitting function of h :

$$c_1 = k_1 \ln h + \mu_1, \quad (7)$$

and β_0 , β_1 , β_2 , k_1 , and μ_1 are fitting parameters.

The new model was tested using the following algorithm. First, values of θ known for a particular date from ground measurements or other sources were substituted into Equations (3) and (4) to determine b and c . Then, the obtained values of b and c were substituted into Equation (2) to determine h . Finally, the determined values of h were substituted into Equations (6) and (7) to determine b_1 and c_1 , which in turn were used in Equation (5) to retrieve θ on any other date for which σ_{vv} is known.

2.2. Study area

The study area was located in the Besor River basin (Northern Negev desert, Israel), with the focus on the Secher stream catchment. Four test sites (1 ha) were selected in which the undisturbed land consisted of either broad valleys surrounded by hills (sites 1 and 2), or broad alluvial valleys with terrace systems (sites 3 and 4). Each site was uniform in terms of surface soil colour and texture, characterized by flat topography, and devoid of vegetation due to lack of soil moisture. Sites 1 (farm Zeelim, latitude $31^\circ 10' 53''$ N, longitude $34^\circ 32' 35''$ E) and 2 (farm Rivivim, $31^\circ 07' 28''$ N, $34^\circ 37' 50''$ E) were on sandy Aridisols and sites 3 (farm Wadi Mashash, $30^\circ 04' 13''$ N, $34^\circ 50' 49''$ E) and 4 (farm Wadi Mashash, $30^\circ 04' 21''$ N, $34^\circ 51' 32''$ E) were on sandy loam soils along the Nahal Secher Stream. Classification and properties of soils on the test sites are presented in Table 1.

The study comprised the years 1996, 1997, 1998, and 2000. Rainfall during the wet period (November–May) was 100–140 mm, whereas rainfall during the dry period (June–October) was absent. The average soil temperature at a depth of 1–2 cm varies between 15 and 30°C , and soil water content is insufficient for plant growth most of the year. During the wet period, θ reaches the maximum of 30% by volume in sandy loam and 20% by volume in sand.

Table 1. Classification and properties of soils on the research sites.

Site	Soil type	Taxonomy	Parent materials	Physiography	Texture			Bulk density (kg m^{-3})
					Clay (%)	Silt (%)	Sand (%)	
1 and 2	Sand	Aridisols	Sand	Broad valleys surrounded by hills	4	8	88	1670
3 and 4	Sandy loam	Aridisols	Loess, sand	Broad alluvial valleys with terrace systems	15	30	55	1460

2.3. ERS-2 SAR data

For this project, four ERS-2 archival SAR images were obtained from the European Space Agency. ERS-2 is the follow-on mission to ERS-1 and was launched in 1995. The images were provided in precision image (PRI) format with a pixel spacing of 12.5 m. The ERS-2 SAR sensor operates at the C-band (operating wavelength $\lambda = 5.65$ cm) vertically co-polarized with an image centre incidence angle of 23° (reference incident angle). The same orbit is repeated every 35 days. There was an overlap of ascending (south–north) and descending (north–south) scenes within 12.5 h over the region of interest. In this study, descending scenes obtained at 10:00 a.m. LST (local standard time) on 23 May 1996, 22 August 1997, 24 April 1998, 25 December 1998, and 24 March 2000 were used. All images were geometrically transformed to the Universal Transverse Mercator (UTM) coordinate system by ERDAS IMAGINE software (version 8.5; Intergraph Corporation, Huntsville, AL, USA) using ground control points. Then, to identify the research sites on the imagery, the ground-determined coordinates (using a GPS receiver) of the sites were applied. For each site, the backscattering coefficients of pixels were calculated and corrected for variation in incident angle using the equations of Laur et al. (2004). The local incidence angle, θ_1 , for each individual pixel was calculated using the geometry of the SAR and topographic information using the expression given by Robinson (1966).

Each 1 ha test site was represented by an 8×8 neighbourhood of 64 pixels on an ERS SAR image. The σ_{vv}^0 data obtained over the four test sites were filtered by a 5×5 pixel median filter to reduce speckle noise. Average values of backscattering coefficients, σ_{vv}^0 , were calculated for each test site and used for further retrieval of h and θ (Table 2).

2.4. Determination of roughness

In December 2000, three-dimensional surface roughness was directly measured within each site using an automated surface roughness profiler, BGU GSS1800, developed at the remote sensing laboratory, Department of Geography and Environmental Development, Ben Gurion University of the Negev (Blumberg et al. 2002; Blumberg, Freilikher, Ben-Asher, et al. 2006). The profiler integrates a laser source, charge-coupled device (CCD) camera, onboard central processing unit (CPU), and encoder, mounted on a tripod and positioned at a distance of 2.0 m from the scanned area. The device scans by moving along a fixed horizontally positioned rail. The laser illuminates a line (length 60 cm) on the soil surface while the CCD camera captures the laser reflection from the surface. After each scan, the rail automatically rotates around a vertical axis at an angle of 1° to perform the next scan (i.e. the total number of scans on each plot is 360). The CPU and encoder determine the offset of the laser beam and generate a digital file with the values for elevation

Table 2. Mean values of backscattering coefficient σ_{vv}^0 , (dB) obtained over the research sites reduced to $\theta_1 = 23^\circ$.

Site	Soil type	Date of survey				
		23 May 1996	22 August 1997	24 April 1998	25 December 1998	24 March 2000
1	Sand	-17.13	-23.34	-20.8	-22.34	-17.58
2	Sand	-17.27	-22.35	-19.9	-21.77	-20.55
3	Sandy loam	-15.96	-21.12	-19.7	-20.08	-19.68
4	Sandy loam	-17.46	-20.62	-19.9	-19.86	-16.18

at a height resolution of 0.015 cm and spacing of 0.5 cm. The area captured is a circle of diameter 1.2 m, with an enclosed square of 0.84×0.84 m.

The data scanned by BGU GSS1800 were then reduced to RMS height h and correlation length l (Blumberg and Freilikhler 2001) for all 64 pixels, and mean h and l were then calculated for each test site. As an isotropic surface is independent of azimuth, h could be calculated in one dimension (Verhoest et al. 2008).

Retrieving of h for a given soil type was carried out using Equations (2), (3), and (4) for known σ_{vv}^0 , θ_1 , θ , and T . Values of l were calculated according to Equation (1) using retrieved values of h . Retrieval of mean values of h for each site was based on mean values of σ_{vv}^0 obtained for both the dry and wet periods and the known values of θ to verify their temporal stability.

2.5. Determination of soil water content

SAR observation depth (i.e. thickness of the top soil layer influencing the backscattering signal) is important for the verification of retrieved θ by direct ground measurements. Considering the dielectric properties of soil, the observation depth Z increases with increase in λ and decrease in θ . According to Walker et al. (1997, 2004) and Owe and Van de Griend (1998), Z varies from 0.1 to 0.25λ (cm) depending on soil moisture content. Since the λ of ERS-2 SAR is 5.65 cm, the practical limit for soil water content in the arid region under study was retrieved at a depth of 1–2 cm. During the dry period, the retrieved value for θ was also valid for depths up to 6 cm, since θ was uniform up to this depth (Carmi and Berliner 2008).

Ground reference measurements of soil water content θ_g were performed using the following methods.

- (1) Time domain reflectometry (TDR) with 5 cm probes, allowing *in situ* measurements. This method was used for most measurements of θ_g .
- (2) Gravimetric method: weighing the wet soil samples, drying them in an oven at 105°C for 24 h, and then re-weighing them. Obtained gravimetric θ_g was then converted to volumetric θ_g using soil bulk density values. This method was used only for control and TDR calibration in order to avoid overestimation typical of TDR (Bittelli, Salvatorelli, and Rossi Pisa 2008).

At each test site, 64 measurements of θ_g were obtained (one for each pixel of the satellite image), and then the mean value $\bar{\theta}_g$ was calculated. According to Agam and Berliner (2004), θ is uniformly low in the study area during the dry period. Based on field measurements at the time of the satellite survey (10:00 a.m. LST), the values of θ in the top 1 cm of soil were highly invariant ($1 \pm 0.1\%$ by volume for sites 1 and 2, and $2.3 \pm 0.2\%$ by volume for sites 3 and 4). Therefore, during the dry period, θ could be considered as known and labour-intensive ground measurements for the retrieval of h were not required.

As a control during the wet period, $\bar{\theta}_g$ of each test site was also determined by TDR within 2 h of the satellite survey. Since during the wet period the variation of θ with time was not negligible, the measured values of θ_g were interpolated to match the time of the survey. Interpolation was accomplished by linear regression in MS Excel, with time as an independent variable.

Relative errors ($\delta_\theta = \Delta\theta/\theta$) of $\bar{\theta}_g$ did not exceed ± 0.1 at the confidence level of 95%. Retrieval of θ for each soil type under known σ_{vv}^0 , θ_1 , h , and T was carried out using Equations (5), (6), and (7) described in Section 2.1. Retrieved soil water content for one

pixel was defined as θ_r . The mean value of soil water content for each test site $\bar{\theta}_r$ was retrieved using the corresponding average value of σ_{vv}^0 .

2.6. Error analysis

According to Equations (2) and (5), the absolute error $\Delta\sigma_{vv}^0$ for determination of σ_{vv}^0 leads to absolute errors in the retrieved values of roughness, Δh_{σ^o} , and soil water content, $\Delta\theta_{\sigma^o}$. Then, using Equations (2) and (5), Δh_{σ^o} and $\Delta\theta_{\sigma^o}$ can be presented as (Taylor 1997)

$$\Delta h_{\sigma^o} = \frac{\partial h}{\partial \sigma_{vv}^0} \Delta \sigma_{vv}^0 = bh \Delta \sigma_{vv}^0, \quad (8)$$

$$\Delta \theta_{\sigma^o} = \frac{\partial \theta}{\partial \sigma_{vv}^0} \Delta \sigma_{vv}^0 = b_1 \theta \Delta \sigma_{vv}^0. \quad (9)$$

Accordingly, the relative errors δh_{σ^o} and $\delta \theta_{\sigma^o}$ are

$$\delta h_{\sigma^o} = \frac{\Delta h_{\sigma^o}}{h} = b \Delta \sigma_{vv}^0, \quad (10)$$

$$\delta \theta_{\sigma^o} = \frac{\Delta \theta_{\sigma^o}}{\theta} = b_1 \Delta \sigma_{vv}^0. \quad (11)$$

Analysis of Equations (10) and (11) reveals that δh_{σ^o} and $\delta \theta_{\sigma^o}$ are proportional to σ_{vv}^0 and do not depend on the absolute values of h and θ .

Using Equations (2)–(4), the absolute error of retrieved h caused by the absolute error of determination of θ can be presented as

$$\Delta h_{\theta} = \frac{\partial h}{\partial \theta} \Delta \theta = kbh \theta^{-1} \Delta \theta + (\alpha_1 + 2\alpha_2 \theta) b^{-1} h \ln(h) \Delta h. \quad (12)$$

Using Equations (5)–(7), the absolute error of retrieved θ caused by the absolute error of determination of h can be presented as

$$\Delta \theta_h = \frac{\partial \theta}{\partial h} \Delta h = k_1 b_1 \theta h^{-1} \Delta h + (\beta_1 + 2\beta_2 h) b_1^{-1} \theta \ln(\theta) \Delta h. \quad (13)$$

In Equations (12) and (13), Δh and $\Delta \theta$ are absolute errors of ground measurements of h and θ ; α_0 , α_1 , α_2 , k , μ , β_0 , β_1 , β_2 , k_1 , and μ_1 are the same fitting parameters as in Equations (3), (4), (6), and (7). Fitting parameters for the two different soil textures under $\theta_1 = 23^\circ$ and $T = 20^\circ\text{C}$ are presented in Table 3.

Table 3. Parameters for the Equations (3), (4), (6) and (7) under $\theta_1 = 23^\circ$ and $T = 20^\circ\text{C}$.

Soil type	α_0 (dB ⁻¹)	α_1 (dB ⁻¹ (vol%) ⁻¹)	α_2 (dB ⁻¹ (vol%) ⁻²)	k (dB)	μ (dB)	β_0 (dB ⁻¹)	β_1 (dB ⁻¹ cm ⁻¹)	β_2 (dB ⁻¹ cm ⁻²)	k_1 (dB)	μ_1 (dB)
Sand	0.07	14.00×10^{-5}	-1.83×10^{-6}	-1.98	9.57	0.42	0.15	-0.05	-14.31	9.47
Sandy loam	0.07	9.43×10^{-5}	-3.98×10^{-7}	-2.35	11.53	0.34	0.11	-0.04	-14.45	11.84

Thus, the relative errors of retrieved h and θ can be presented as

$$\delta h_\theta = \frac{\Delta h_\theta}{h} = kb\theta^{-1} \Delta\theta + (\alpha_1 + 2\alpha_2\theta) b^{-1} \ln(h)\Delta\theta, \quad (14)$$

$$\delta\theta_h = \frac{\Delta\theta_h}{\theta} = k_1 b_1 h^{-1} \Delta h + (\beta_1 + 2\beta_2 h) b_1^{-1} \ln(\theta)\Delta h. \quad (15)$$

According to Taylor (1997), if the errors in σ_{vv}^0 and θ are independent and random, then the total absolute error, $\Delta h_{\sigma^\circ\theta}$, and relative determination error, $\delta h_{\sigma^\circ\theta}$, can be presented as

$$\Delta h_{\sigma^\circ\theta} = \sqrt{\Delta h_{\sigma^\circ}^2 + \Delta h_\theta^2} = \sqrt{(bh\Delta\sigma_{vv}^0)^2 + (kbh\theta^{-1}\Delta\theta + (\alpha_1 + 2\alpha_2\theta) b^{-1}h \ln(h)\Delta\theta)^2}, \quad (16)$$

$$\delta h_{\sigma^\circ\theta} = \sqrt{\delta h_{\sigma^\circ}^2 + \delta h_\theta^2} = \sqrt{(b\Delta\sigma_{vv}^0)^2 + (kb\theta^{-1}\Delta\theta + (\alpha_1 + 2\alpha_2\theta) b^{-1} \ln(h)\Delta\theta)^2}. \quad (17)$$

In the same way, if the errors in σ_{vv}^0 and h are independent and random, then the total absolute error, $\Delta\theta_{\sigma^\circ h}$, and relative determination error, $\delta\theta_{\sigma^\circ h}$, can be presented as

$$\Delta\theta_{\sigma^\circ h} = \sqrt{\Delta\theta_{\sigma^\circ}^2 + \Delta\theta_h^2} = \sqrt{(b_1\theta\Delta\sigma_{vv}^0)^2 + (k_1 b_1 \theta h^{-1} \Delta h + (\beta_1 + 2\beta_2 h) b_1^{-1} \theta \ln(\theta)\Delta h)^2}, \quad (18)$$

$$\delta\theta_{\sigma^\circ h} = \sqrt{\delta\theta_{\sigma^\circ}^2 + \delta\theta_h^2} = \sqrt{(b_1\Delta\sigma_{vv}^0)^2 + (k_1 b_1 h^{-1} \Delta h + (\beta_1 + 2\beta_2 h) b_1^{-1} \ln(\theta)\Delta h)^2}. \quad (19)$$

As calculations show, the contribution of the term $(\alpha_1 + 2\alpha_2\theta)b^{-1} \ln(h)\Delta\theta$ in the value of $\delta h_{\sigma^\circ\theta}$ was 1.6% for sand and 2.5% for sandy loam, while the contribution of the term $(\beta_1 + 2\beta_2 h)b^{-1} \ln(\theta)\Delta h$ in the value of $\delta\theta_{\sigma^\circ h}$ was 2.7% for sand and 3.2% for sandy loam. This means, that $\delta h_{\sigma^\circ\theta}$ and $\delta\theta_{\sigma^\circ h}$ are almost independent from h and θ , and can be expressed by the following simplified equations:

$$\delta h_{\sigma^\circ\theta} = \sqrt{\delta h_{\sigma^\circ}^2 + \delta h_\theta^2} \approx \sqrt{(b\Delta\sigma_{vv}^0)^2 + (kb\theta^{-1}\Delta\theta)^2}, \quad (20)$$

$$\delta\theta_{\sigma^\circ h} = \sqrt{\delta\theta_{\sigma^\circ}^2 + \delta\theta_h^2} \approx \sqrt{(b_1\Delta\sigma_{vv}^0)^2 + (k_1 b_1 h^{-1} \Delta h)^2}. \quad (21)$$

3. Results and discussion

Comparison with the data from the roughness profiler allowed evaluation of the retrieval accuracy of h and l . The difference between retrieved and measured mean values of h did not exceed 0.017 cm (4.1%) for sand and 0.025 cm (5.6%) for sandy loam (Table 4).

In Table 4, the difference between mean values of h retrieved during the wet and dry periods did not exceed 0.014 cm (3.5%) for sand and 0.020 cm (4.4%) for sandy loam. These values are close to the relative errors for the retrieval of h calculated using Equation (20) (3.8% for sand and 3.9% for the sandy loam), which are shown in Table 5.

The general stability of h under arid conditions was proved by the small standard deviation (SD) of retrieved h during the whole period of surveillance: SD = 0.007 cm (1.8%)

Table 4. Retrieved and measured values of h (cm) and l (cm) over the four research sites.

Site	Soil type	Retrieved for 23 May 1996		Retrieved for 22 August 1997		Retrieved for 24 April 1998		Retrieved for 25 December 1998		Retrieved for 24 March 2000		Measured on 17–20 December 2000	
		h (cm)	l (cm)	h (cm)	l (cm)	h (cm)	l (cm)	h (cm)	l (cm)	h (cm)	l (cm)	h (cm)	l (cm)
1	Sand	0.387	6.6	0.390	6.6	0.393	6.7	0.390	6.6	0.404	6.8	0.406	6.7
2	Sand	0.386	6.6	0.396	6.7	0.402	6.8	0.384	6.5	0.385	6.6	0.387	4.6
3	Sandy loam	0.432	7.3	0.441	7.4	0.43	7.2	0.440	7.4	0.419	7.1	0.444	8.7
4	Sandy loam	0.433	7.3	0.457	7.6	0.431	7.3	0.446	7.5	0.464	7.7	0.447	8.4

Table 5. Relative errors for the RMS height h , calculated using Equations (10), (14), and (20) for two different soil textures.

Soil type	$\Delta\sigma_{vv}^{0*}$ (dB)	θ (%) by vol.)	b (dB ⁻¹)	kb	$\Delta\theta$ (%) by vol.)	Relative errors for h		
						δh_{σ_0}	δh_{θ}	$\delta h_{\sigma_0\theta}$
Sand	± 0.5	1.00%	0.0708	-0.14	± 0.10	± 0.035	± 0.014	± 0.038
Sandy loam	± 0.5	2.30%	0.0706	-0.166	± 0.20	± 0.035	± 0.017	± 0.039

* After 3×3 median filtration

Table 6. Mean remotely retrieved θ_r and mean ground measured θ_g on the four research sites (% by vol.).

Site	Soil type	23 May 1996		24 April 1998		25 December 1998		24 March 2000	
		$\bar{\theta}_r$ (%) by vol.)	$\bar{\theta}_g$ (%) by vol.)	$\bar{\theta}_r$ (%) by vol.)	$\bar{\theta}_g$ (%) by vol.)	$\bar{\theta}_r$ (%) by vol.)	$\bar{\theta}_g$ (%) by vol.)	$\bar{\theta}_r$ (%) by vol.)	$\bar{\theta}_g$ (%) by vol.)
1	Sand	15.2	14.0	1.6	2.0	1.3	1.7	12.3	14.3
2	Sand	12.9	13.2	3.1	2.7	1.5	1.7	2.8	3.2
3	Sandy loam	18.4	19.0	4.0	4.4	3.9	3.7	4.5	5.7
4	Sandy loam	8.6	10.5	3.1	4.0	3.5	3.7	14.1	13.1

for sand and SD = 0.013 cm (3.1%) for sandy loam. These results confirm the suitability of the approach proposed. As can be seen from Table 4, the difference between calculated and measured mean values of l ($\leq 40\%$) was much greater than that for h , reportedly because of difficulties in obtaining ground measurements of l (Baghdadi et al. 2004).

As values of θ_r and θ_g at the wet period were affected by the specific weather conditions during the survey, the increased values of θ_r and θ_g on 23 May 1996 and 24 March 2000 are explained by rainfall, high air humidity, reduced solar radiation, and dew on the eve of the survey (Table 6).

In Table 6, the differences in θ among sites during the wet period demonstrate the uneven distribution of precipitation, which is typical for the Northern Negev desert. Low

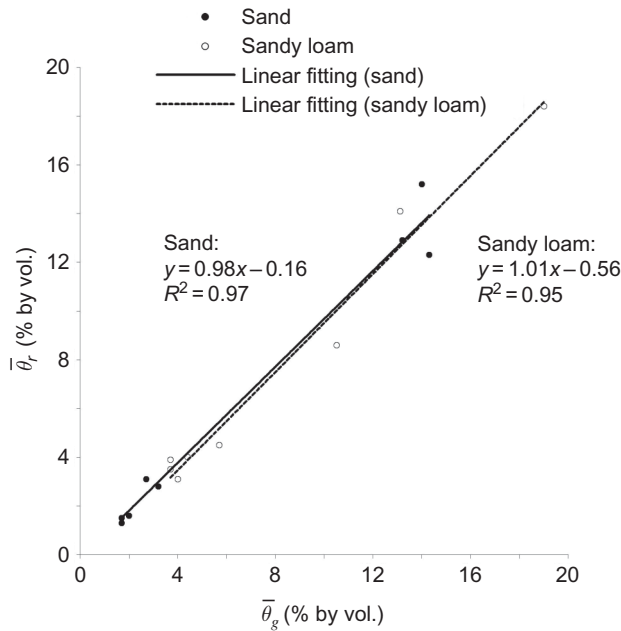


Figure 1. Comparison of mean soil water content, θ_r , retrieved from mean values of σ_{vv}^0 , derived from SAR imagery on 23 May 1996, 24 April 1998, 25 December 1998, and 24 March 2000 and soil mean water content, θ_g , measured on two sandy and two sandy loam sites.

Table 7. Relative errors for the surface soil water content θ , calculated using Equations (11), (15) and (21) for two different soil textures.

Soil type	$\Delta\sigma_{vv}^{0*}$ (dB)	h (cm)	b_1 (dB ⁻¹)	$k_1 b_1$	Δh (cm)	Relative errors for θ		
						$\delta\theta_{\sigma^0}$	$\delta\theta_h$	$\delta\theta_{\sigma^0 h}$
Sand	± 0.5	0.4	0.469	6.709	± 0.015	± 0.234	± 0.251	± 0.343
Sandy loam	± 0.5	0.45	0.378	5.461	± 0.018	± 0.189	± 0.218	± 0.288

Note: *After 3x3 median filtration

$\bar{\theta}_r$ and $\bar{\theta}_g$ on 24 April 1998 and 25 December 1998 are explained by the absence of precipitation during these months.

A scatter plot between retrieved $\bar{\theta}_r$ and directly measured $\bar{\theta}_g$ demonstrates a strong linear relationship, with a slope near unity and intercept near zero (Figure 1).

The relative error of $\bar{\theta}_r$ was 0.15 for sandy soils and 0.13 for sandy loam soils. Averaging decreased the relative error, $\delta\bar{\theta}_r$, 2.3-fold in comparison with $\delta\theta_{\sigma^0 \theta}$ for a single pixel (Table 7). This confirms the ability of the method proposed for the retrieval of θ and the effectiveness of 64 pixel averaging for reduction of $\Delta\theta_r$ and $\delta\theta_r$.

At the same time, while averaging led to a deterioration in spatial resolution in the mapping of θ , the use of the 5×5 pixel median filter on σ_{vv}^0 for each site pixel alleviated this problem. For example, to obtain the distribution of θ_r at site 4, filtered values of σ_{vv}^0 derived from the remote data survey of 24 March 2000 were used. The necessary values of h for each pixel of the site were also calculated using corresponding filtered values of σ_{vv}^0 derived from the remote data surveyed on 22 August 1997 (dry period) under $\theta = 2.3\%$

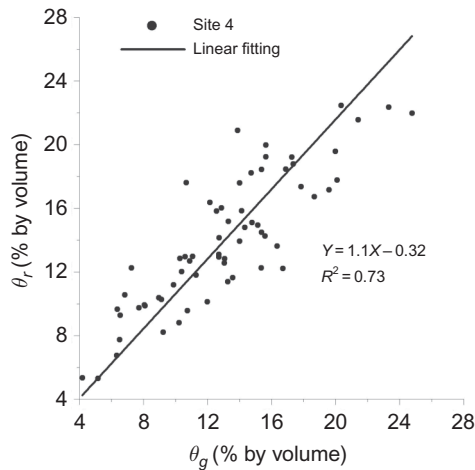


Figure 2. Comparison of soil water content, θ_r , retrieved from filtered values of σ_{vv}^0 , derived from SAR imagery obtained on 24 March 2000 and soil water content θ_g , measured on site 4.

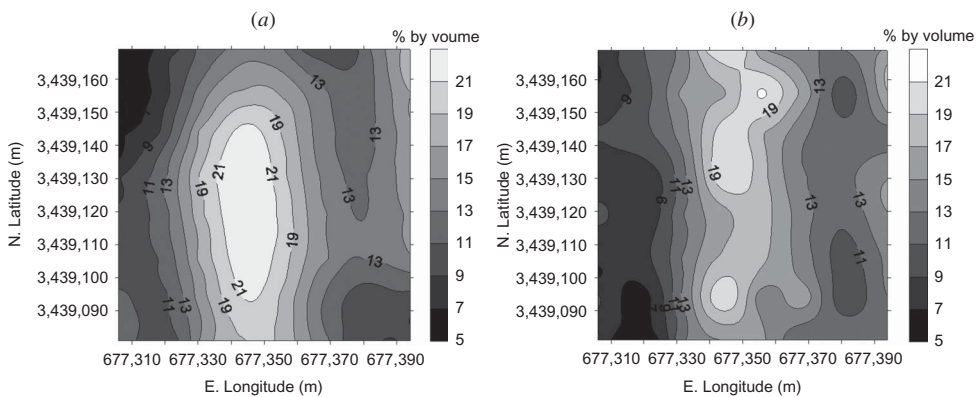


Figure 3. (a) Distribution of soil water content, θ_r (% by vol.), retrieved from values of σ_{vv}^0 , derived from SAR imagery obtained on 24 March 2000 for site 4; (b) Distribution of soil water content, θ_g (% by vol.), measured on the same site on the same date.

by volume. The values of θ_r were then calculated as described in Section 3.4. *In situ* TDR measurements of θ_g compare well with the retrieved values of θ_r for site 4 (Figure 2).

Correlation between θ_r and θ_g is lower than that between $\bar{\theta}_r$ and $\bar{\theta}_g$, due to filtering, but is adequate for mapping purposes. At 0.153, the value of $\delta\theta_r$ calculated as $\delta\theta_r = RMSe/\bar{\theta}_r$, is 1.9-fold less than $\delta\theta_{\sigma_{vv}^0}$ calculated for one pixel (Table 7). For the sandy sites, $\delta\theta_r$ was reduced twice due to filtering.

The main advantage of the median filtering method is its ability to reduce $\delta\theta_r$ while the spatial resolution of θ_r mapping remains practically the same. Visual comparison of maps of θ_r and θ_g for site 4 shows that the spatial distribution of our radar-retrieved θ is similar to *in situ* measurements of θ (Figure 3).

A map of θ_r distribution within the Wadi Mashash catchment is shown in Figure 4.

Parameter θ_r was retrieved from σ_{vv}^0 derived from remote sensing imagery on March 24 2000. The values of h for each pixel were calculated using σ_{vv}^0 from remote sensing on

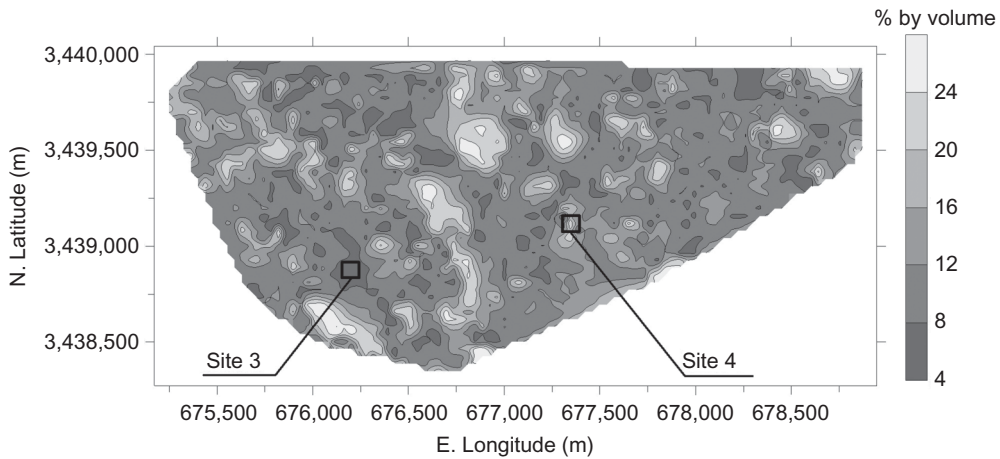


Figure 4. Distribution of soil water content, θ_r (% by vol.), retrieved from values of σ_{vv}^0 , derived from SAR imagery obtained on 24 March 2000 within the Wadi Mashash catchment.

August 22 1997. Rainfall occurred one day before the survey on 23 March 2000, and thus the heterogeneous distribution of θ_r shown in Figure 4 may be due to lateral redistribution and accumulation of water in the topographically variable conditions. The mean value of θ_r over the whole area was 12.2% by volume, with higher values (16–24% by volume) found between stream banks and lower values (4–8% by volume) in upper slope positions.

4. Summary and conclusions

The new algorithm for retrieving surface roughness and soil water parameters was successfully applied to ERS-2 imagery of undisturbed lands in the Negev desert of Israel. The importance of the method proposed for retrieval of θ and h lies in its ability to model h and θ as functions of σ_{vv}^0 for soils with little roughness, provided one of the two parameters is known. Furthermore, this study demonstrated the possibility of concurrent determination of h and θ from single-channel ERS data using specific conditions of an arid environment.

Analysis of variations of θ and h showed that θ remained practically constant at the time of survey ($\pm 0.2\%$ by volume) during the dry period, and variation in h was less than 3% during the whole observation period. Therefore, our assumption that surface roughness does not change significantly over time and that surface water content varies insignificantly during the dry season was correct, and our method is deemed warranted.

Error analysis of the proposed algorithm showed that the relative determination errors of h and θ were not dependent on their absolute values. To reduce these errors, methods of averaging and median filtering of σ_{vv}^0 were tested. Averaging over an 8×8 neighbourhood of 64 pixels reduced the relative error of retrieved θ by a factor of 2.3, at the expense of spatial resolution. In comparison, application of a moving 5×5 median filter reduced $\delta\theta_r$ 2-fold while maintaining spatial resolution. Retrieved h and θ obtained after averaging and filtering of σ_{vv}^0 were in agreement with ground reference measurements.

The numerical analysis demonstrated low sensitivity of σ_{vv}^0 to l within the range 2–20 cm typical of many natural surfaces. This suggests that Equation (1) is usable for any type of soil without a significant error increase. Although this study focused on only two soil types, the results are sufficiently promising to suggest that the method described is

applicable to any soil in an arid environment. In addition, the method proposed will be suitable for processing data from other radar satellites, including the European Space Agency's Envisat and the Canadian Space Agency's Radarsat-2.

Acknowledgements

This work was supported by Israel's Space Agency and Ministry of Science under National Strategic Infrastructure Grant no. 1368. In addition, a number of archival images were made available by European Space Agency Grant no. AO3-222.

References

- Agam, N., and P. R. Berliner. 2004. "Diurnal Water Content Changes in the Bare Soil of a Coastal Desert." *Journal of Hydrometeorology* 5: 922–933.
- Álvarez-Mozos, J., J. Casali, M. Gonzalez-Audicana, and N. E. C. Verhoest. 2006. "Assessment of the Operational Applicability of RADARSAT-1 Data for Surface Soil Moisture Estimation." *IEEE Transactions on Geoscience and Remote Sensing* 44: 913–924.
- Baghdadi, N., M. Aubert, O. Cerdan, L. Franchistéguy, C. Viel, E. Martin, M. Zribi, and J. F. Desprats. 2007. "Operational Mapping of Soil Moisture Using Synthetic Aperture Radar Data: Application to the Touch Basin (France)." *Sensors* 7: 2458–2483.
- Baghdadi, N., O. Cerdan, M. Zribi, V. Véronique Auzet, F. Frédéric Darboux, M. Hajj, and R. B. Kheir. 2008. "Operational Performance of Current Synthetic Aperture Radar Sensors in Mapping Soil Surface Characteristics in Agricultural Environments: Application to Hydrological and Erosion Modeling." *Hydrological Processes* 22: 9–20.
- Baghdadi, N., I. Gherboudj, M. Zribi, M. Sahebi, C. King, and F. Bonn. 2004. "Semi-empirical Calibration of the IEM Backscattering Model Using Radar Images and Moisture and Roughness Field Measurements." *International Journal of Remote Sensing* 25: 3593–3623.
- Baghdadi, N., N. Holah, and M. Zribi. 2006. "Soil Moisture Estimation Using Multi-Incidence and Multi-Polarization ASAR SAR Data." *International Journal of Remote Sensing* 27: 1907–1920.
- Bindlish, R., and A. P. Barros. 2000. "Multifrequency Soil Moisture Inversion from SAR Measurements with the Use of IEM." *Remote Sensing of Environment* 71: 67–88.
- Bittelli, M., F. Salvatorelli, and P. Rossi Pisa. 2008. "Correction of TDR-Based Soil Water Content Measurements in Conductive Soils." *Geoderma* 143: 133–142.
- Blumberg, D. G., and V. Freilikhher. 2001. "Soil Water-Content and Roughness Retrieval Using ERS-2 SAR Data in the Negev Desert, Israel." *Journal of Arid Environments* 49: 449–464.
- Blumberg, D. G., V. Freilikhher, J. Ben-Asher, J. Daniels, Y. Kaganovskii, A. Kotlyar, and L. Vulfson. 2006. "Microwave Subsurface Remote Sensing in the Negev Desert: Soil Moisture Detection." *Waves in Random and Complex Media* 16: 179–203.
- Blumberg, D. G., V. Freilikhher, Y. Kaganovskii, and A. Maradudin. 2002. "Subsurface Microwave Remote Sensing of Soil-Water Content: Field Studies in the Negev Desert and Optical Modeling." *International Journal of Remote Sensing* 19: 4039–4054.
- Blumberg, D. G., and R. Greeley. 1993. "Field Studies of Aerodynamic Roughness Length." *Journal of Arid Environments* 25: 39–48.
- Blumberg, D. G., G. Ronen, J. Ben-Asher, V. Freilikhher, L. Vulfson, and A. Kotlyar. 2006. "Utilizing a P-Band Scatterometer to Assess Soil Water Saturation Percent of a Bare Sandy Soil." *Journal of Hydrology* 318: 374–378.
- Blyth, K. 1997. "An Assessment of the Capabilities of the ERS Satellites' Active Microwave Instruments for Monitoring Soil Moisture Change." *Hydrology and Earth System Sciences* 1: 159–174.
- Carmi, G., and P. Berliner. 2008. "The Effect of Soil Crust on the Generation of Runoff on Small Plots in an Arid Environment." *Catena* 74: 37–42.
- Dubois, P. C., J. Van Zyl, and T. Engman. 1995. "Measuring Soil Moisture with Imagine Radars." *IEEE Transactions on Geoscience and Remote Sensing* 33: 916–926.
- Fung, A. K. 1994. *Microwave Scattering and Emission Models and their Applications*, 373–385. London: Artech House.
- Fung, A. K., and K. S. Chen. 2004. "An Update of the IEM Surface Backscattering Model." *IEEE Geoscience and Remote Sensing Letters* 1: 75–77.

- Gherboudj, I., M. Ramata, A. A. Berg, and B. Toth. 2011. "Soil Moisture Retrieval over Agricultural Fields from Multi-Polarized and Multi-Angular RADARSAT-2 SAR Data." *Remote Sensing of Environment* 115: 33–43.
- Laur, H., P. Bally, P. Meadows, J. Sanchez, B. Schaettler, E. Lopinto, and D. Esteban. 2004. "ERS SAR Calibration: Derivation of the Backscattering Coefficient σ^0 in ESA ERS SAR PRI Products." Doc. ES-TN-RS-PM-HL09, Issue 2, Revision 5f: 3–5.
- Lin, D. S. 1994. "On the Suitability of Field Surface Roughness Measurements as Input to Microwave Backscattering Models." In *Proceedings of the First Workshop on Data Collection and Data Analysis Issues for Spatial and Temporal Soil Moisture Mapping from ERS-1 and JERS-1 SAR Data and Macroscale Hydrologic Modeling (EV5V-CT94-0446)*, 91–98. Naples: Institute for Agricultural Hydraulics, University of Naples.
- Moran, M. S., D. C. Hymer, J. Qi, and E. E. Sano. 2000. "Soil Moisture Evaluation Using Multi-Temporal Synthetic Aperture Radar (SAR) in Semiarid Rangeland." *Agricultural and Forest Meteorology* 105: 69–80.
- Oh, Y., K. Sarabandi, and F. T. Ulaby. 1992. "An Empirical Model and an Inversion Technique for Radar Scattering from Bare Soil Surfaces." *IEEE Transactions on Geoscience and Remote Sensing* 30: 370–381.
- Oh, Y., K. Sarabandi, and F. T. Ulaby. 1994. "An Inversion Algorithm for Retrieving Soil Moisture and Surface Roughness from Polarimetric Radar Observation." In *Proceedings, International Geoscience and Remote Sensing Symposium (IGARSS)*, 1582–1584. Pasadena, CA: IEEE.
- Owe, M., and A. A. Van de Griend. 1998. "Comparison of Soil Moisture Penetration Depths for Several Bare Soils at Two Microwave Frequencies and Implications for Remote Sensing." *Water Resources Research* 34: 2319–2327.
- Peplinski, N. R., F. T. Ulaby, and M. C. Dobson. 1995. "Dielectric Properties of Soils in the 0.3–1.3 GHz Range." *IEEE Transactions on Geoscience and Remote Sensing* 33: 803–807.
- Rees, W. G., and N. S. Arnold. 2007. "Scale-dependent Roughness of a Glacier Surface: Implications for Radar Backscatter and Aerodynamic Roughness Modelling." *Journal of Glaciology* 52: 214–222.
- Robinson, N. 1966. *Solar Radiation*, 35–38. Amsterdam: Elsevier.
- Sud, Y. C., P. J. Sellers, Y. Mintz, M. D. G. K. Chou Walker, and W. E. Smith. 1990. "Influence of the Biosphere on the Global Circulation and Hydrologic Cycle—A GCM Simulation Experiment." *Agricultural and Forest Meteorology* 52: 133–180.
- Taylor, J. R. 1997. *An Introduction to Error Analysis: The Study of Uncertainties in Physical Measurements*, 73–77. Sausalito, CA: University Science Books.
- Thoma, D. P., M. S. Moran, R. Bryant, M. Rahman, C. D. Holifield Collins, S. Skirvin, E. E. Sano, and K. Slocum. 2006. "Comparison of Four Models to Determine Surface Soil Moisture from C-Band Radar Imagery in a Sparsely Vegetated Semiarid Landscape." *Water Resources Research* 42: 1–12.
- Ulaby, F. T., R. K. Moore, and A. K. Fung. 1986. *Microwave Remote Sensing: Active and Passive, Vol. 3: From Theory to Applications: 1817–1822*. Boston, MA: Artech House.
- Verhoest, N. E. C., H. Lievens, W. Wagner, J. Álvarez-Mozos, M. S. Moran, and F. Mattia. 2008. "On the Soil Roughness Parameterization Problem in Soil Moisture Retrieval of Bare Surfaces from Synthetic Aperture Radar." *Sensors* 8: 4213–4248.
- Verhoest, N. E. C., P. A. Troch, C. Paniconi, and F. P. de Troch. 1998. "Mapping Basin Scale Variable Source Areas from Multitemporal Remotely Sensed Observations of Soil Moisture Behavior." *Water Resources Research* 34: 3235–3244.
- Walker, J. P., R. Paul, P. R. Houser, R. Garry, and G. R. Willgoose. 2004. "Active Microwave Remote Sensing for Soil Moisture Measurement: A Field Evaluation Using ERS-2." *Hydrological Processes* 18: 1975–1997.
- Walker, J. P., P. A. Troch, M. Mancini, G. R. Willgoose, and J. D. Kalma. 1997. "Profile Soil Moisture Estimation Using the Modified IEM." *IEEE Geoscience and Remote Sensing Letters* 7: 1263–1265.
- Zribi, M., N. Baghdadi, N. Holah, and O. Fafin. 2005. "New Methodology for Soil Surface Moisture Estimation and its Application to ENVISAT-ASAR Multi-Incidence Data Inversion." *Remote Sensing of Environment* 96: 485–496.